Investigation of Al,Si order in K-feldspars using ^{27}Al and ^{29}Si MAS NMR

YUEHUI XIAO, R. JAMES KIRKPATRICK, RICHARD L. HAY, YOUN JOONG KIM

Dept. of Geology, University of Illinois, Urbana, IL 61801, USA

AND

BRIAN L. PHILLIPS

Division of Materials Science and Engineering, University of California, Davis, CA 95616, USA

Abstract

This paper presents a ^{27}Al and ^{29}Si MAS NMR study of K-feldspars and demonstrates that the spectra are sensitive to variations in the state of Al,Si order. For synthetically annealed samples, the results are in agreement with previous IR spectroscopy (Harris *et al.*, 1989) and demonstrate that Al,Si rearrangement continues after the samples have become monoclinic as determined by powder XRD. NMR methods provide a significantly improved picture of the state of local Al,Si order in such samples. For triclinic samples, measures of the state of Al,Si order (M1 and M2 of ^{27}Al spectra and M2 of ^{29}Si spectra) correlate well with site occupancies determined by powder XRD, but for the monoclinic samples the NMR parameters continue to change whereas the XRD parameters do not. Interpretations based on the NMR results for the synthetically disordered samples are consistent with 1-step disordering, as observed by XRD. ^{27}Al and ^{29}Si MAS NMR is likely to be a useful tool for probing the state of local Al,Si order in a wide variety of natural samples.

KEYWORDS: Al,Si order, K-feldspars, nuclear magnetic resonance.

Introduction

TRADITIONAL interpretations concerning the tetrahedral site occupancies of alkali feldspars are primarily based on correlations between Al/Si ratio on a given site and mean T–O distance determined by diffraction methods (Smith, 1974). These interpretations are ultimately the basis for all optical and cell-parameter methods for determining the degree of Al,Si ordering currently in use (Wright and Stewart, 1968; Steward and Ribbe, 1969; Kroll, 1971, 1973; Kroll and Ribbe, 1983). The primary weakness of this approach is that there is no fundamental theory relating the mean interatomic distances in disordered structures to site occupancies. Thus, the assumption of linearity between lattice parameters of the geometrically averaged structure and the local degree of Al,Si order is not necessarily true (Eggleton and Buseck, 1980; Ribbe, 1983).

This paper presents the results of a study of the Al,Si order in a series of synthetically annealed, K-exchanged Amelia albite samples and natural, authigenic K-feldspars using ^{27}Al and ^{29}Si MAS NMR in conjunction with powder XRD and TEM. The purpose of this study is to provide measures of the local degree of Al,Si order independent of the assumptions of XRD analysis, to compare the results to previous infrared spectroscopy (Harris *et al.*, 1989) and, thus, to understand better Al,Si order in alkali feldspars.

The degrees of Al,Si order determined from NMR and XRD for our monoclinic K-feldspars are different and are potentially significant because of the common occurrence of alkali feldspars and their use in interpreting geological environments and thermal history (Smith, 1974; Kroll and Ribbe, 1983; Hay *et al.*, 1988; Kroll and Knitter, 1991). The observed differences between the NMR and XRD results have their origin in the differences between the length scales probed by the two methods and the effects of structural modulations for those samples that contain them. Unit cell parameters

Mineralogical Magazine, March 1995, Vol. 59, pp. 47–61

TABLE 1*a*. XRD cell parameters

Sample	*a*	*b*	*c*	α	β	γ	*V*	B‡
Kat-0	8.590(2)	12.981(2)	7.226(1)	90.64(1)	115.91(1)	87.65(1)	724.2(1)	2.39(2)
Kat-1	8.594(1)	12.977(2)	7.219(1)	90.61(2)	115.97(1)	87.92(2)	723.3(2)	2.11(2)
Kat-2	8.603(3)	12.986(4)	7.209(2)	90.35(3)	115.98(2)	88.58(4)	723.8(3)	1.45(4)
Kat-5	8.604(2)	13.022(3)	7.201(2)	90.24(3)	116.01(2)	89.14(2)	725.0(2)	0.87(4)
Kat-10	8.609(2)	13.037(3)	7.187(2)	90.04(2)	116.00(2)	89.96(2)	725.0(2)	0.04(4)
Kat-20	8.603(2)	13.041(3)	7.186(2)	90.04(3)	116.01(2)	90.04(2)	724.5(3)	0.07(2)
Kat-33	8.608(2)	13.036(2)	7.182(1)	89.99(2)	116.02(1)	90.04(2)	724.3(2)	0.03(2)
Kat-62	8.613(1)	13.047(2)	7.186(2)	90.04(3)	116.00(1)	90.01(2)	725.8(2)	0.05(1)
Kat-92	8.614(2)	13.046(3)	7.185(2)	90.02(3)	116.03(1)	90.01(2)	725.6(3)	0.03(1)
Bt-1	8.582(3)	12.926(5)	7.219(2)	90.60(3)	115.93(3)	87.88(3)	719.7(3)	2.15(4)
Drk4	8.610(3)	13.009(4)	7.194(2)	90.00(3)	115.98(3)	90.03(4)	724.3(3)	0.04(4)
Kfstpt	8.607(3)	13.035(6)	7.196(2)	89.95(4)	116.07(3)	89.93(5)	725.2(4)	0.11(3)

‡ Obliquity B = arccos (sinα sinγ*).

TABLE 1*b*. XRD parameters

(Al site occupancy are calculated from powder XRD using the method of Kroll and Ribbe (1983)).

Sample	t1o+t1m	t1o–t1m	t1o	$\sigma^{1/2}$	$\tau^{1/2}$	M1†	M2†
Kat-0	0.98(1)	1.01(1)	1.00(1)	1.03(3)	0.96(2)	29.75(4)	0.165(5)
Kat-1	0.94(1)	0.88(1)	0.91(1)	0.94(3)	0.88(2)	29.75(5)	0.122(4)
Kat-2	0.85(2)	0.58(2)	0.72(2)	0.68(4)	0.70(3)	29.74(6)	0.074(4)
Kat-5	0.71(2)	0.34(2)	0.53(2)	0.48(2)	0.42(3)	29.73(9)	0.048(4)
Kat-10	0.60(2)	0.02(2)	0.31(2)	0.03(2)	0.20(4)	29.74(10)	0.018(3)
Kat-20	0.58(2)	−0.01(2)	0.28(2)	−0.02(2)	0.16(4)	29.74(7)	0.010(2)
Kat-33	0.57(1)	−0.01(1)	0.28(1)	−0.02(1)	0.14(2)	29.74(10)	0.006(3)
Kat-62	0.57(1)	−0.01(1)	0.28(1)	−0.02(1)	0.14(2)	29.74(10)	0.006(3)
Kat-92	0.57(2)	−0.00(2)	0.28(2)	−0.00(2)	0.14(2)	29.74(7)	0.008(2)

† First and second moments of 131–1$\bar{3}$1 peak(s).

TABLE 1*c*. NMR parameters

Sample	t1o	$\sigma^{1/2}$ 1-step	$\sigma^{1/2}$ 2-step	$\tau^{1/2}$ 1-step	$\tau^{1/2}$ 2-step	$M1_{(Si)*}$	$M2_{(Si)*}$	$M1_{(Al)*}$	$M2_{(Al)*}$
Kat-0	1.00	1.00	1.00	1.00	1	−97.7(6)	6.3(3)	54.68(6)	5.7(3)
Kat-1	0.87	0.91	0.74	0.83	1	−97.9(5)	7.6(2)	55.32(6)	8.7(3)
Kat-2	0.71	0.76	0.42	0.61	1	−98.1(4)	9.8(3)	55.67(9)	12.4(5)
Kat-5	0.58	0.61	0.16	0.33	1	−98.1(4)	10.7(2)	56.23(8)	13.8(4)
Kat-10	0.42	0.37	0	0.23	0.68	−98.3(4)	13.2(4)	56.83(5)	15.0(3)
Kat-20	0.30	0.13	0	0.07	0.20	−98.5(3)	14.6(5)	57.03(7)	15.2(3)
Kat-33	0.28	0.08	0	0.04	0.12	−98.7(4)	15.6(5)	57.21(6)	15.8(3)
Kat-62	0.28	0.08	0	0.04	0.12	−98.8(3)	15.5(4)	57.09(6)	16.6(3)
Kat-92	0.28	0.08	0	0.04	0.12	−98.6(4)	15.7(3)	57.14(9)	16.0(5)

* First and second moment of ^{29}Si and ^{27}Al NMR spectra.

determined from powder XRD data are averages over volumes with characteristic lengths of hundreds of Å. In the presence of structural modulations, the unit cell parameters are averages over several wavelengths of the modulations (Xu *et al.*, 1989). They depend not only on the geometry of individual unit cells, but also on the development of the modulation (Eggleton and Buseck, 1980; Böhm, 1983; Kim, 1989). The NMR chemical shift and QCC, on the other hand, depend primarily on local (NN and NNN) structure and composition. The observed spectrum is the sum of the signal from all the nuclei in the sample, and the relative intensity at a given frequency reflects the fraction of the nuclei giving rise to that chemical shift. Thus, although the average unit cell parameters of different samples may be the same they may have different degrees of short-range Al,Si order and yield different NMR spectra. Therefore, the degree of short-range Al,Si order and macroscopic changes in unit cell geometry are not necessarily directly proportional to each other. This situation is quite similar to that observed for ordering of Mg-cordierite (Putnis and Bish, 1983; Putnis and Angel, 1985; Putnis *et al.*, 1987; Salje, 1987), except that our synthetic samples are undergoing disordering. NMR has proven to be a useful tool for investigating the local structures of many kinds of feldspar (Lippmaa *et al.*, 1980; K. A. Smith *et al.*, 1983; J. V. Smith *et al.*, 1984; Kirkpatrick *et al.*, 1985; Sherriff and Hartman, 1985; Yang *et al.*, 1986; Kirkpatrick *et al.*, 1987; Kirkpatrick, 1988; Phillips *et al.*, 1988).

Investigation of intermediate-composition alkali feldspars using the NMR methods described here is possible using K-exchanged samples. Na,K occupancy of the alkali sites causes loss of spectral resolution and changes in the chemical shifts (Kirkpatrick *et al.*, 1985; Sherriff and Hartman, 1985; Phillips *et al.*, 1988). We have examined samples of albite which were synthetically disordered and then K-exchanged (work in progress) which yield NMR spectra essentially identical to those of the K-feldspars described here.

Experimental

Samples. The synthetic K-feldspar samples was prepared by hand-picking clean fragments of Amelia albite and ion-exchanging them in molten KCl at 805°C for 48 hours. Three exchanges under these conditions gave a fine powder of microcline with Or content greater than 99%, as confirmed by XRD and ^{29}Si and ^{23}Na NMR. These microcline samples were then annealed isothermally at 1093 (±3)°C for times up to 92 days (Table 1). Each annealed sample consisted of about 1 gram of powder wrapped in Pt foil. After annealing, the samples were quenched in air.

The authigenic samples are from a variety of localities (Bt-1, Green River Formation, WY, USA; K5205, unknown locality; Drk4, Deicke Formation, IA, USA; Kfstpt, St. Peter Formation, WI, USA) and were chosen to represent a range of Al,Si order. These samples consist mostly of K-feldspar grains *c.* 1–5 μm across. K5205, Drk4, Kfstpt contain a small amount of clay minerals. XRD shows that K5205 is a mixture of ordered and disordered K-feldspar.

Powder X-ray Diffraction. All samples were mixed with annealed CaF_2 as an internal standard and examined by powder XRD using a Siemens model D500/501 diffractometer with a graphite monochrometer under the following conditions: 30 kV, 30 mA, 0.01°/step over the 2θ range 10° to 70°. Peaks were indexed following Borg and Smith (1969). Unit-cell parameters were determined by least-square refinement using the LCLSQ program of Burnham (1962) with Cu-$K\alpha_1$ 1.540598 Å.

NMR spectroscopy. The ^{27}Al magic angle spinning (MAS) NMR spectra were obtained at 130.3 MHz using a 'home-built' spectrometer with a 11.7T superconducting solenoid (Oxford Instruments) and a Nicolet 1280 data acquisition system. The samples were spun at ~10 kHz using a 5 mm MAS probe manufactured by Doty Scientific (Columbia, SC). Short radio frequency pulses (1 μs; solution $\pi/2$ ~6.5 μs) were used to uniformly excite the central transition of ^{27}Al. Delay times between acquisitions were 1 s. About 800 scans were collected for each spectrum. The ^{27}Al chemical shifts are reported in ppm from external 1 *M* $AlCl_3$ solution.

The ^{29}Si MAS NMR spectra were collected at 71.5 MHz using a similar spectrometer with a 8.45T superconducting magnet. The samples were spun at ~4 kHz using a 7 mm Doty Scientific probe. The radio frequency pulse was 4μs ($\pi/4$ flip angle), and 400 s delay time was used due to the extremely long T_1 in these samples. Chemical shifts are reported relative to external tetramethylsilane (TMS).

Transmission electron microscopy. Flake specimens of kat-5 (annealed for 4.8 days, Table 1) were made by the conventional method of crushing grains to obtain very thin cleavage flakes. These flakes were obtained from the powder used in the X-ray study. Small amounts of these powders were further crushed in pure acetone with an agate mortar and pestle. The fine particles were dispersed ultrasonically in acetone and mounted on Formvar-supported holey copper grids. In order to avoid imaging overlapped flakes, only single flakes were chosen and studied. An Hitachi model 600 (100 kV) microscope was used for imaging and diffraction work. An attached energy dispersive X-ray analyser (model TN-5500) was used to determine the microchemistry of the flakes.

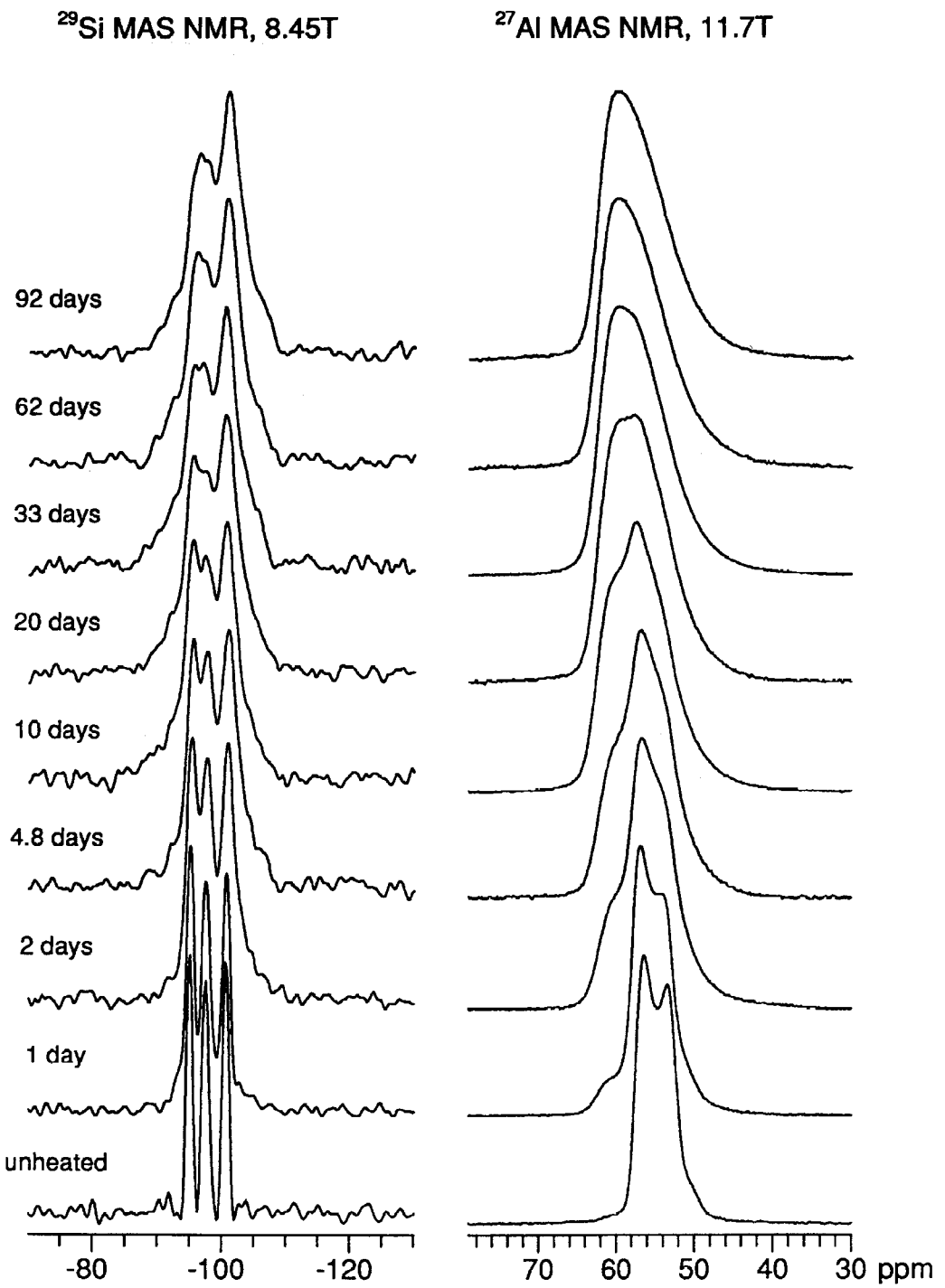

FIG. 1. ^{29}Si and ^{27}Al MAS NMR spectra of the laboratory annealed K-feldspar samples.

Results and spectral simulation

Synthetic samples. The ^{29}Si MAS NMR spectra of the synthetic samples (Fig. 1) show a systematic change from three narrow peaks for the unannealed samples to several broad peaks and shoulders for the longest annealed samples. The three peaks for the unannealed sample are at −95.2 ppm; −97.7 ppm; −100.8 ppm, essentially the same chemical shifts previously reported for maximum microcline (J.V. Smith *et al.*, 1984; Kirkpatrick *et al.*, 1985). They correspond to Si on T2m (Q^4(2Al)), T2o (Q^4(1Al)) and T1m (Q^4(1Al)), respectively. Qualitatively, the most important change in these spectra with increasing annealing time are: (1) the peaks broaden; (2) resolution between, especially, the peaks for Si on T2o and T2m decreases; (3) the relative intensity of the peak near −100.8 ppm increases; and (4) new peaks and shoulders appear at about −106.0 ppm, −104.0 ppm, −92.3 ppm and −89.5 ppm. These additional peaks and shoulders indicate the formation of additional local tetrahedral environments (Q^4(nAl), n = 0,1,2,3,4) due to Al,Si disordering. Resolution in these spectra is better than in those of Sherriff and Hartman (1985), possibly because their samples contained some albite.

Simulation of these ^{29}Si spectra with individual peaks is not unique because there are 20 possible Si environments (4 T sites × 5 NNN environments), but the broadening can be quantitatively described by the second moment of the spectra, M2, defined as

$$M_2 = \frac{\int_0^\infty (\omega - \langle\omega\rangle)^2 f(\omega) d\omega}{\int_0^\infty f(\omega) d\omega}, \qquad (1)$$

where $f(\omega)$ is relative intensity at given frequency ω, and $\langle\omega\rangle$ is the first moment (centre of gravity, hereafter called M1) of the spectrum (Slichter, 1990). The second moment more usefully describes the shape of a spectrum than the Full Width at Half-Height (FWHH), because it is sensitive to the relatively low intensity shoulders formed due to disordering, whereas the FWHH is not.

The second moments of the ^{29}Si spectra (Table 1, Fig. 2) change continuously from 6.3 ppm^2 for the unannealed sample to 15.7 ppm^2 for the 92-day sample.

The first moments (mean chemical shifts) of the ^{29}Si spectra also appear to change systematically but vary only from −97.7(6) ppm to −98.8(3) ppm, nearly within the error of measurement.

Like the ^{29}Si spectra, the ^{27}Al MAS NMR spectra (Fig. 1) show systematic peak broadening and loss of resolution with increasing annealing time. Because of unaveraged second-order quadrupole broadening, however, separate peaks for Al on different sites are not as well resolved. The spectrum of the unannealed sample is a second order quadrupole powder pattern with an isotropic chemical shift (δ_i) of 58.7 ppm, a quadrupole coupling constant (QCC) of 3.2 MHz and an asymmetry parameter (η) of 0.2, in good agreement with previous work (Kirkpatrick *et al.*, 1985, Phillips *et al.*, 1988). There is also a small amount of intensity at ~60 ppm which increases continuously with increasing annealing time. The main peak is readily assigned to Al on

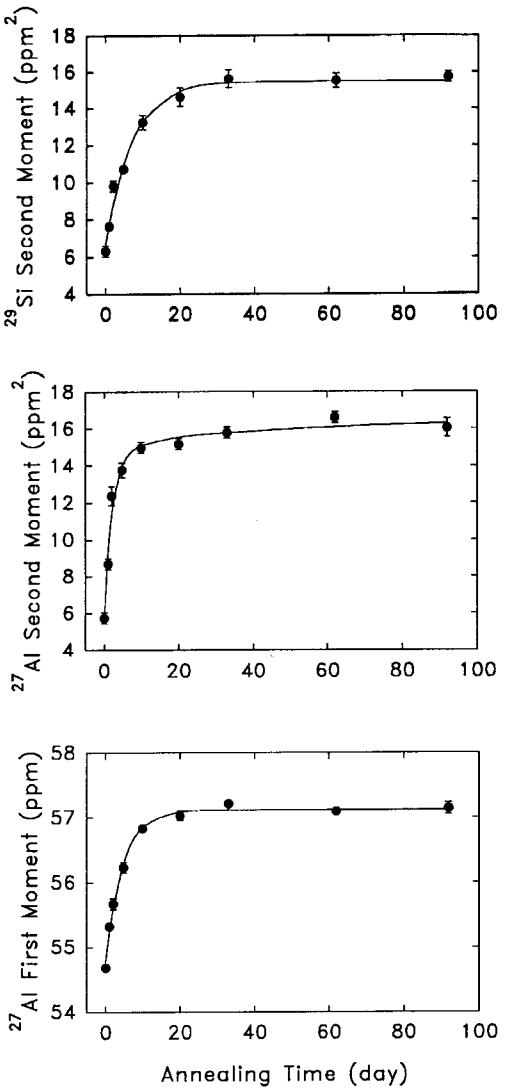

FIG. 2. Variation of the ^{27}Al first moment (M1) and second moment M2 and the ^{29}Si M2 from the MAS NMR spectra of the laboratory annealed samples with annealing time.

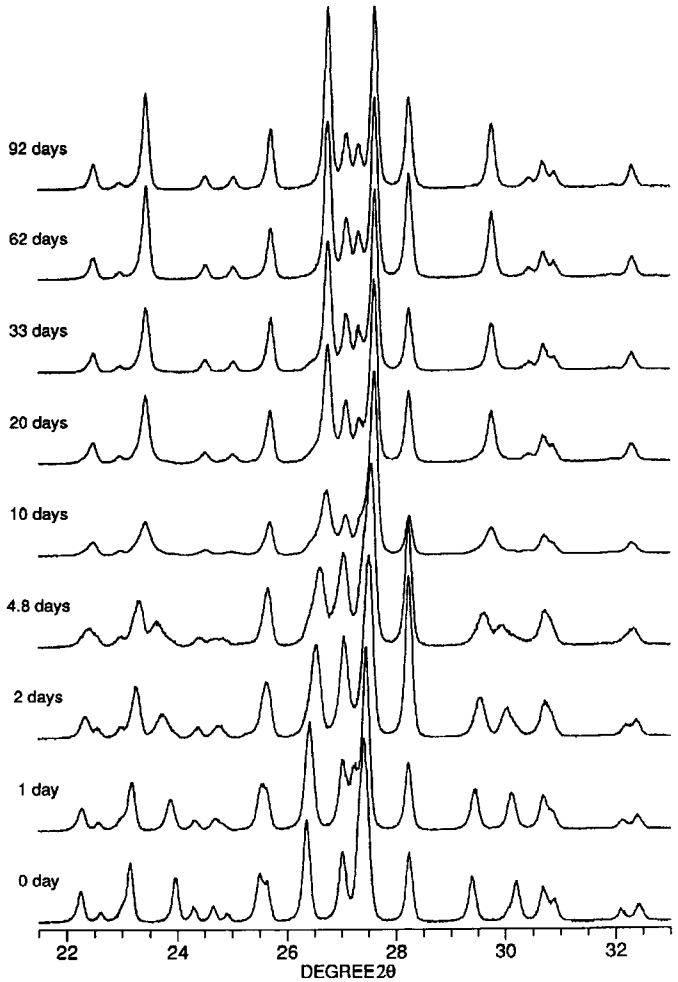

FIG. 3. Powder XRD patterns for the synthetic samples.

T1o of microcline and the increasing intensity at ~60 ppm is assigned to Al on sites other than T1o. There is also a small amount of intensity at ~53 ppm that can not be simulated well by these two components. The origin for this low frequency tail is unknown, but may be due to inhomogeneous broadening from a distribution of δ_i, QCC and η and/or a minor amount of impurity. Observation of the spinning sidebands arising from the $\pm(\frac{3}{2} \leftrightarrow \frac{1}{2})$ ^{27}Al transition (Samoson, 1985; Phillips *et al.*, 1987, 1988) was tried, but resolution is not improved relative to that for the $(\frac{1}{2} \leftrightarrow -\frac{1}{2})$ central peak.

The M1 and M2 values of the ^{27}Al spectra both increase continuously with increasing annealing time (Fig. 2, Table 1). The origin of these changes is clearly the increase in intensity with a maximum in the 60 ppm range. There is little increase in intensity at chemical shifts more negative than the peak for Al on T1o, and at least for annealing times of 10 days and less the peaks are clearly the sum of the peak for Al on T1o and the broader peak centred at about 60 ppm for Al on T1m, T2o and T2m. Separate features for Al on these sites cannot be resolved at this H_0 field strength. Thus, we take the fractional relative height at 60.2 ppm compared to that of the longest annealed sample as a measure of the T1o occupancy (Table 1). 60.2 ppm is the peak maximum of the longest annealed sample. The T1o occupancies for the samples with longer annealing times obtained by this method are likely to be less accurate than those

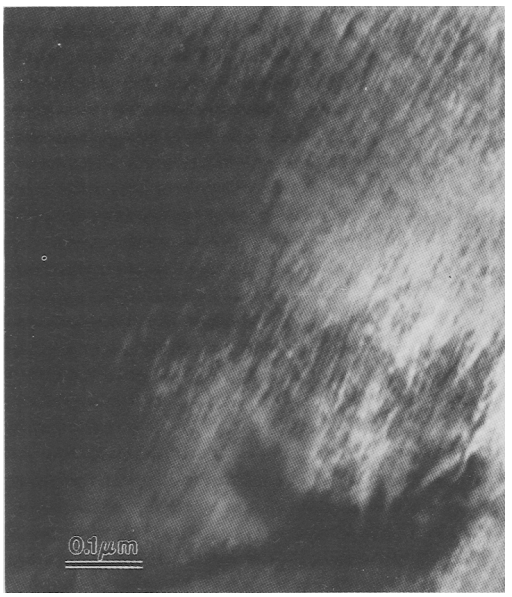

FIG. 4. TEM bright field image of the 4.8 days laboratory annealed sample. Tweed structure is present on a scale of ~100 Å.

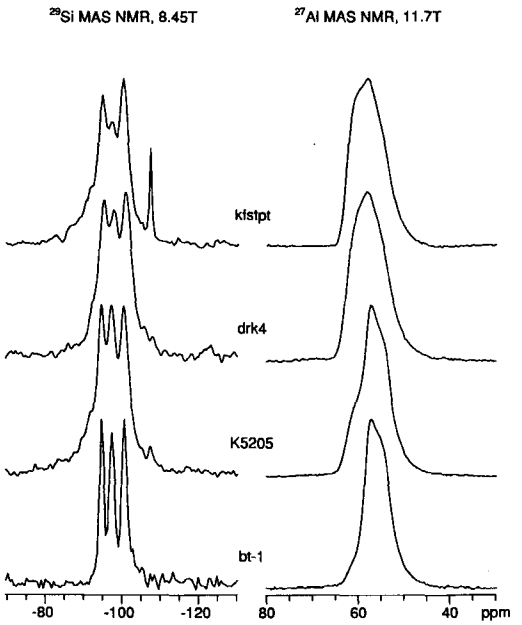

FIG. 5. ^{29}Si and ^{27}Al MAS NMR spectra of authigenic K-feldspars.

with shorter annealing times, but we show below that they correlate well with the values obtained from XRD for the triclinic samples.

We have also attempted to simulate the spectra using our fitting routine which specifies isotropic chemical shift, quadrupole coupling constant, and asymmetry parameter (QVAS, Phillips *et al.*, 1988) with a component similar to the peak for Al on T1o in ordered microcline and a broader component for Al on the other three sites. These values agree with the values from the peak height method to within 10%, but because of the peak overlap the results are subjective. The chemical shifts, quadrupole coupling constants, asymmetry parameters, and line-broadening functions are variable parameters, and a variety of fits simulate the spectra satisfactorily.

As expected, the lattice parameters and the Al contents of the T1o site calculated from the *b*, *c*, α^* and β^* lattice parameters vary systematically with annealing time (Fig. 3 and Table 1; see Kroll and Ribbe, 1983; Stewart and Ribbe, 1969). Based on the centroids of the diffraction peaks, the samples annealed for 10 days or longer are monoclinic, and those annealed for shorter times are triclinic. Careful examination of the 29.0 to 31.5° 2θ region of the diffraction patterns (Fig. 3) shows that the (131) peak for the monoclinic samples does not become fully narrowed until the 33-day sample, and the (131) and ($1\bar{3}1$) peaks for the 1, 2, and 4.8-day samples are broadened compared to the unannealed sample. Thus, the structures of the 1, 2, 4.8, 10 and possibly the 20-day samples are locally heterogeneous. The M2 value of this peak or pair of peaks decreases from 0 to 33-days of annealing, whereas the first moment remains unchanged (Table 1).

Tweed structures are present in TEM images of most of the flakes of the one sample we examined (4.8 days). This tweed structure has modulated image contrast in two directions with a periodicity of 100–200 Å in both directions (Fig. 4). The image contrast, however, is weak compared to that of Amelia albite samples annealed at 1073°C (Kim, 1989). This microstructure is also electron-beam sensitive, and the images disappear rapidly on exposure to the electron beam. Microchemical analysis of each grain which showed tweed structure shows the presence of only Al, Si and K, indicating that only K-feldspar grains were examined.

Similar tweed structures are commonly observed in intermediate K-feldspars (Eggleton and Buseck, 1980; Xu *et al.*, 1989), and based on the broadened XRD peaks, we expect that the samples annealed for 1, 2, 10 and perhaps 20 days also have tweed structures.

Authigenic K-feldspar samples. The ^{27}Al and ^{29}Si NMR spectra of the authigenic samples we have examined are similar to those of the synthetic

samples (Fig. 5), except for ^{29}Si signal for quartz near −107.3 ppm in the K5205 and Kfstpt samples and ^{29}Si signal for phyllosilicates in the −80 to −93 ppm range for the K5205, Drk4, and Kfstpt samples. The ^{27}Al signal for the phyllosilicates is well out of the range of interest here (near 0 ppm), because the Al is all octahedrally coordinated. The presence of the ^{29}Si signal for the quartz and clays prevents quantitative use of its M2 values for these spectra, but the ^{27}Al spectra can be used quantitatively. As for the synthetic samples, the more disordered samples have broader ^{29}Si peak envelopes, and the ^{27}Al signal for Al not on T1o occurs in the −60 ppm region. Since there are not enough data points, we do not make correlations for these authigenic samples.

Discussion

XRD. As expected from previous studies (e.g. Goldsmith and Laves, 1954; Sipling and Yund, 1974; Smith, 1974; Ribbe, 1983; Blasi *et al.*, 1984), the XRD data indicate that the Al,Si disordering in our synthetic samples is taking place by a so-called 1-step path. In such a path Al on T1o moves equally into the three other T-sites. In contrast, in an ideal 2-step process the Al on T1o first moves into T1m until the Al site occupancies of the two sites (t1o and t1m, lower case t's indicate Al site occupancy) are equal to 0.5, and then moves into the T2 sites.

The correlation of the symmetry breaking short-range order parameter, $\sigma = (\frac{t1o-t1m}{t1o+t1m})^2$ and the pseudo-symmetry breaking order parameter $\tau = (\frac{t1-t2}{t1+t2})^2$ (Harris *et al.*, 1989) is nearly linear (Fig. 6), as expected for a 1-step process. Note that there is a considerable gap between the σ and τ values for the clearly triclinic samples (the unheated sample and the three with the shortest heating times) and the samples that appear monoclinic based on the XRD peak centroids (τ and σ = *c.* 0). The broadening of the (131) XRD peak for the 10-day and possibly the 20-day samples, however, indicates that the true state of the Al,Si order in these samples is not τ = σ = *c.* 0.

NMR. The ^{27}Al NMR M1 and M2 values correlate well with the ^{29}Si NMR M2 values (Fig. 7), as expected for parameters which are related to the sum of the NMR signal from the entire range of local tetrahedral sites. The correlations are not linear over the entire range of order. Rather, the data for the triclinic samples fall on one linear relationship and the data for the monoclinic samples on another with a

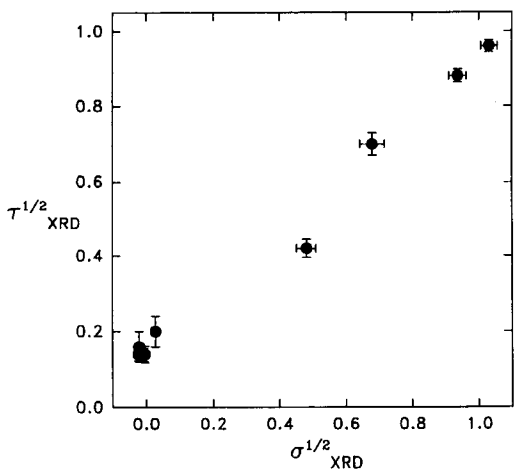

FIG. 6. Correlation of the pseudo-symmetry breaking order parameter $\tau^{1/2}$ from XRD and the symmetry breaking short range order parameter $\sigma^{1/2}$ from XRD.

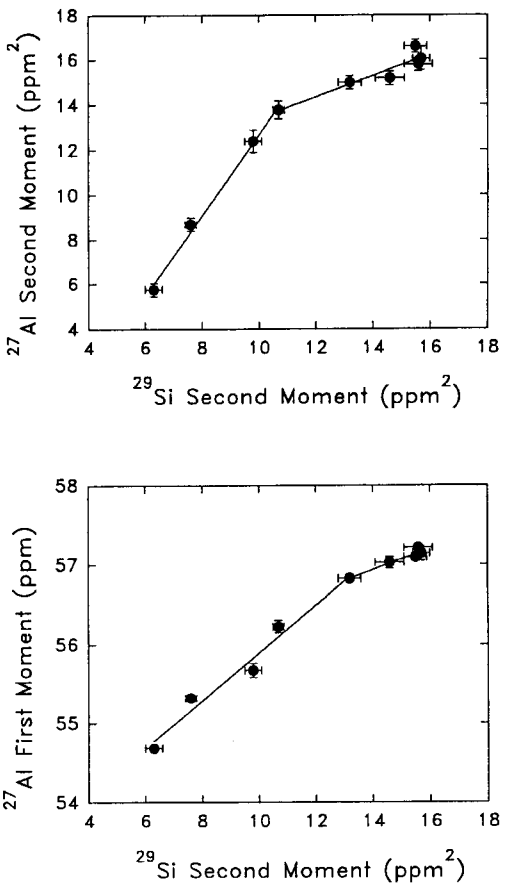

FIG. 7. Correlations of the first moment and second moment of the ^{27}Al MAS NMR peaks with the second moment of the ^{29}Si NMR MAS peaks.

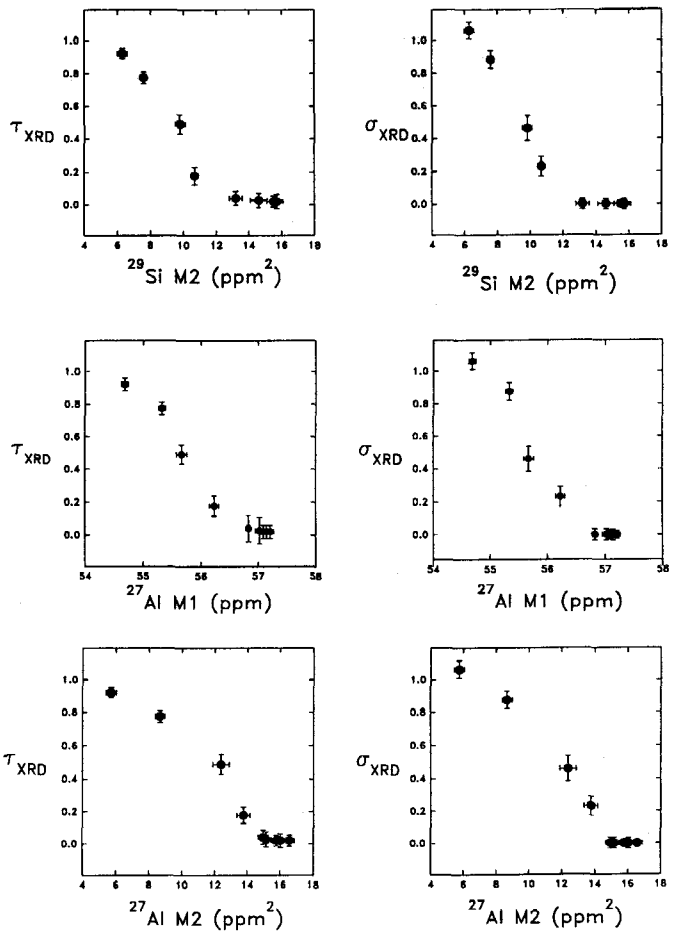

FIG. 8. Correlations of order parameters τ and σ from XRD with ^{27}Al and ^{29}Si NMR moment parameters.

smaller slope. There are probably two factors causing the changes in the slopes. (1) The ^{27}Al M1 and M2 values are probably reflecting primarily the fraction of Al's not on T1o, whereas the ^{29}Si M2 value is probably reflecting this factor plus the details of the Al,Si distribution. For the nearly fully disordered samples, the Al site occupancy may be close to equilibrium, but the changes in the arrangement of the Al's and Si's with respect to each other may not be complete. These changes are likely to be driven by interactions at distances longer than next-nearest neighbour, as in micas and clay minerals (Herrero *et al.*, 1989), and could give rise to changes in the proportions of Q^4(nAl) Si sites, which in turn give rise to changes in the ^{29}Si M2 value. Further investigation of this problem will require modeling of the site occupancies (e.g. Herrero *et al.*, 1989). (2) An additional factor contributing to the change in slope may be an increase in the intensity of the ^{27}Al peak for Al not on T1o at chemical shifts less positive than the peak maximum. This increased intensity would counteract the effect on the ^{27}Al M1 and M2 values from additional Al not on T1o and could be due to an increased average quadrupole coupling constant and/or a less positive isotropic chemical shift for these sites.

Correlation of NMR and XRD results. Harris *et al.* (1989) observed systematic relationships between the positions of certain infrared bands for natural K-rich feldspars and their state of Al,Si order observed by XRD, and we observe similar relationships involving the NMR parameters. Both IR and NMR probe local structure, and similar correlations with Al,Si order are to be expected. Harris *et al.* (1989) argued that the change in IR peak position ($\Delta\omega_i^2$) should be proportional to the short range order parameters σ and τ and a parameter (η) related to local lattice distortions due to the monoclinic–triclinic transition.

$$\Delta\omega_i^2 = \delta_{i,\sigma}\omega + \delta_{i,\eta}\eta + \delta_{i,\tau}\tau \quad (2)$$

They further argued that with respect to the IR results σ could be subsumed into η.

For the NMR M1 and M2 values, we expect the contribution of η to be less than that of σ, because observed changes in ^{29}Si chemical shifts due to occupancy of different sites appears to be greater than changes in the chemical shifts due to lattice distortions. For instance, peak broadening due to Al,Si site disorder for a variety of zeolites is less than the separation between peaks with different numbers of Al NNN (Fyfe *et al.*, 1984). Thus, we expect relationships of the type,

$$M_i \propto C_1\sigma + C_2\tau, \quad (3)$$

where M_i = ^{27}Al M1, ^{27}Al M2, or ^{29}Si M2.

For a 1-step ordering/disordering path σ and τ are proportional to each other (Fig. 6) and both affect the NMR parameters, whereas for a 2-step path the effects of σ dominate at t1o > 0.5 and the effects of τ dominate at t1o < 0.5.

The observed relationships between the three NMR parameters and all measures of the Al,Si order obtained from the peak centroids of the XRD patterns are similar (e.g. Fig. 8) and similar to that between τ and the IR peak positions for natural K-rich feldspars (Harris *et al.*, 1989). The NMR and XRD parameters are proportional to each other for the triclinic samples, but for the monoclinic samples the XRD parameters are constant whereas the NMR parameters continue to change with annealing time.

Because the NMR parameters directly reflect the local Al,Si order, the changing NMR parameters with constant XRD parameters for the monoclinic samples clearly indicates that the samples become sensibly monoclinic without complete Al,Si disorder, as postulated by Harris *et al.* (1989). Thus, the ^{27}Al M1 and M2 and ^{29}Si M2 are more effective measures of the state of Al,Si order in monoclinic K-feldspars than parameters obtained from peak centroids in powder XRD patterns.

Unlike parameters based on XRD peak centroids, the M2 values for the (131)-(1$\bar{3}$1) XRD peaks continue to change somewhat after the peak centroids yield monoclinic symmetry. Even for the (131) M2, however, the values for the longest-annealed samples do not change significantly, whereas the NMR parameters continue to change with long annealing (Fig. 9). The M2 of the XRD (131) peak may be a useful parameter for relatively well ordered sanidines, but apparently does not capture all the changes in Al,Si order for more disordered specimens.

The values of τ and σ obtained from XRD and from the t1o values obtained from ^{27}Al NMR assuming a 1-step disordering path agree with each other well for the triclinic samples, but as expected, the XRD values for the apparently monoclinic samples are 0 whereas the NMR values are greater (Fig. 10). As expected, the τ and σ values calculated from the NMR data assuming a 2-step path do not agree with the XRD results. For a 1-step path, σ can be calculated from the NMR t1o values using the relationship

$$\sigma^{\frac{1}{2}} = \frac{4\ t1o-1}{2\ t1o+1}. \quad (4)$$

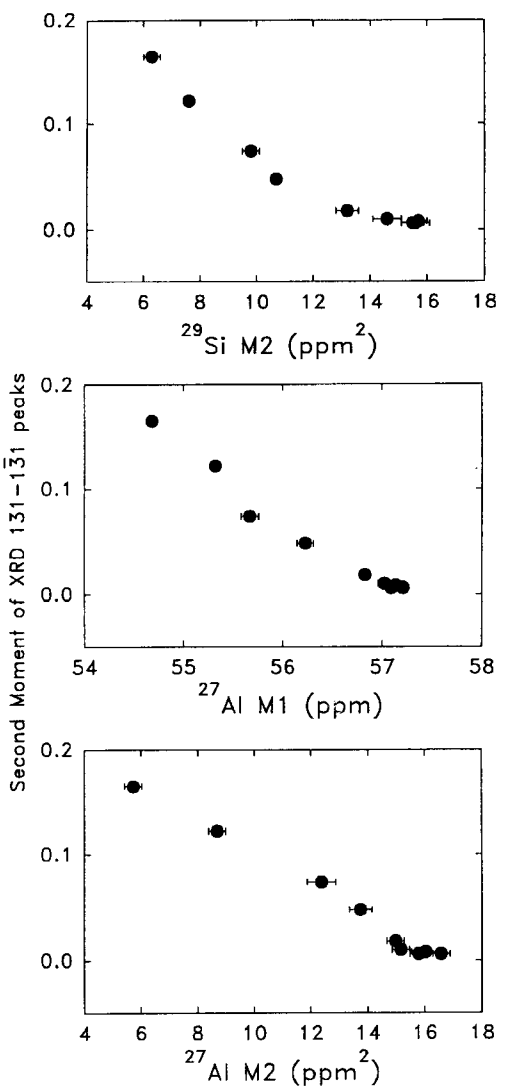

FIG. 9. Correlations of the second moment of the powder XRD 131-1$\bar{3}$1 peaks with ^{27}Al and ^{29}Si NMR moment parameters.

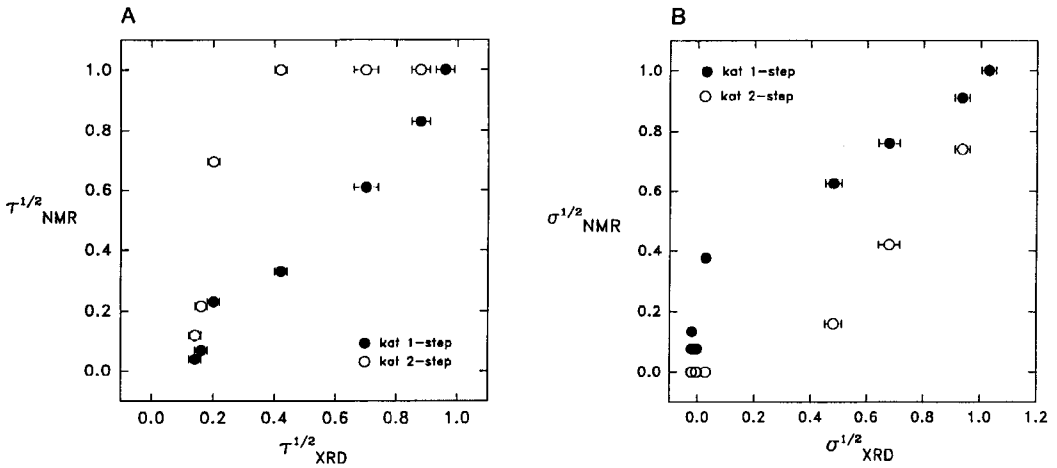

FIG. 10. Correlations of (**A**) the pseudo-symmetry breaking order parameter $\tau^{1/2}$ from NMR and XRD, and **B**) the symmetry breaking short range order parameter $\sigma^{1/2}$ from NMR and XRD. The NMR values are for assumed 1-step and 2-step paths.

TABLE 2. Calculated distributions of local Si environments for 1-step and 2-step models for sample kat-2, which has a t1o occupancy of 0.71 from the ^{27}Al NMR data

Site	1-Step Model	2-Step Model	chemical shift (ppm)
T1o Q^4(4Al)	0.004	0.000	−85.8
T1o Q^4(3Al)	0.029	0.000	−90.8
T1o Q^4(2Al)	0.086	0.000	−95.8
T1o Q^4(1Al)	0.115	0.290	−100.8
T1o Q^4(0Al)	0.057	0.000	−105.8
T1m Q^4(4Al)	0.001	0.000	−85.8
T1m Q^4(3Al)	0.022	0.000	−90.8
T1m Q^4(2Al)	0.188	0.000	−95.8
T1m Q^4(1Al)	0.555	0.710	−100.8*
T1m Q^4(0Al)	0.138	0.000	−105.8
T2o Q^4(4Al)	0.001	0.000	−82.7
T2o Q^4(3Al)	0.022	0.000	−87.7
T2o Q^4(2Al)	0.188	0.206	−92.7
T2o Q^4(1Al)	0.555	0.588	−97.7*
T2o Q^4(0Al)	0.138	0.206	−102.7
T2m Q^4(4Al)	0.006	0.000	−85.2
T2m Q^4(3Al)	0.110	0.146	−90.2
T2m Q^4(2Al)	0.504	0.477	−95.2*
T2m Q^4(1Al)	0.250	0.317	−100.2
T2m Q^4(0Al)	0.033	0.060	−105.2

* indicate the three ^{29}Si peak positions for the unannealed sample.

For a 2-step path the σ values are given by

$$\sigma^{\frac{1}{2}} = 2\ \text{t1o} - 1, \qquad (5)$$

for t1o > 0.5, and σ = 0 by definition for t1o < 0.5.

The attainment of sensibly monoclinic symmetry as detected by the XRD peak centroids without attainment of complete Al,Si disorder also explains the gap in data points between the triclinic and monoclinic samples (e.g. Fig. 6) observed by Harris *et al.* (1989) and us. The actual degree of local Al,Si order, as probed by NMR or IR, is continuous.

Determination of disordering path from ^{29}Si NMR. To increase the ability of NMR spectroscopy to probe the ordering and disordering paths of K-feldspars, we have attempted to simulate the ^{29}Si MAS spectra and compare the calculated and observed spectra. The results show that qualitatively it is possible to distinguish 1-step from 2-step paths, but that quantitative simulation of the spectra will require computer modeling similar to that of, e.g., Herrero *et al.* (1989) for sheet silicates. Difficulties include an unknown change in chemical shift for each NNN Al for Si substitution and the effects of interactions at greater than NNN distances (see Herrero *et al.*, 1989, for a discussion of the possible effects of such interactions on ^{29}Si NMR spectra).

We first calculate the expected distributions of Q^4(nAl) Si sites for each of the four T-sites for both 1-step and 2-step paths and then calculate ^{29}Si NMR spectra based on reasonable assumptions of chemical shifts for these sites. The calculated Al,Si occupancies assume obedience of Loewenstein's Al-O-Al avoidance principle (Loewenstein, 1954). No other

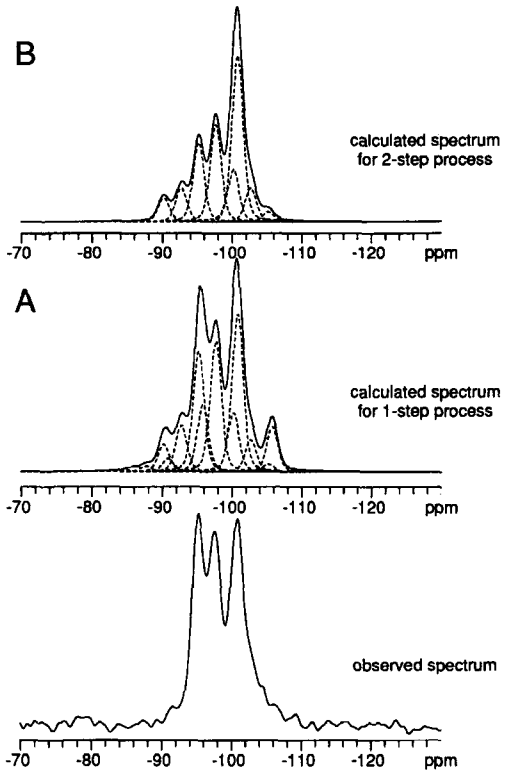

FIG. 11. Observed and calculated ^{29}Si MAS NMR spectra for sample kat-2, which has t1o = 0.71 by ^{27}Al MAS NMR. The calculated spectra assume (**A**) a 1-step disordering path and (**B**) a 2-step disordering path.

restrictions on short-range ordering, such as homogeneous dispersion of charges and maximum dispersion of charges (e.g. Herrero *et al.*, 1989), are included. 1-step disordering is calculated by setting t1m = t2o = t2m for a given value of t1o. 2-step disordering is calculated by setting t2o = t2m = 0 and t1o = t1m for t1o > 0.5, and t1o = t1m and t2o = t2m for t1o < 0.5.

Chemical shifts for different local environments can be estimated from the empirical observation that substitution of an Al NNN for a Si NNN causes an approximately 4 to 5.5 ppm deshielding at ^{29}Si (Lippmaa *et al.*, 1980; Engelhardt *et al.*, 1981; Klinowski *et al.*, 1982; J.V. Smith *et al.*, 1984; Ramdas and Klinowski 1984). Because the ^{29}Si chemical shifts for T2m(2Al), T2o(1Al) and T1m(1Al) are known from the ^{29}Si spectrum of unannealed microcline, the chemical shifts for the other (nAl) environments for these sites can be readily estimated. The chemical shift of ^{29}Si on T1o appears to be approximately the same as for ^{29}Si on T1m, because the peak intensity at the chemical shift of the T1m(1Al) site increases dramatically with annealing. No ordering scheme could cause T1m(1Al) to increase and we assign this intensity to T1o(1Al). Additional support comes from the fact that ⟨T1o-O-T⟩ and ⟨T1m-O-T⟩ become the same with decreasing t1o (Dal Negro *et al.*, 1978).

Comparison of the observed and calculated spectra assuming a 5 ppm change with an Al for Si substitution is consistent with the conclusion from XRD and the NMR moment parameters that disordering is occurring close to a 1-step path. Fig. 11 compares the observed spectrum of sample kat-2 with envelopes calculated for 1-step and 2-step disordering assuming the chemical shifts listed in Table 2, FWHHs of 2 ppm and a fraction Gaussian for each peak = 0.8. The intensity distribution for a 1-step model is very close to the observed spectrum, but that for a 2-step model is very much different. There are two main reasons for this difference. In the 2-step model there is no Al on T2 sites until t1o < 0.5, and thus, no T1 Q^4(2Al) sites would form under these conditions. Si on this site resonates near −96 ppm and the lack of these sites causes the spectral intensity in this region to be much less than in the 1-step model and the observed spectrum. In addition, in the 2-step model the number of T2o Q^4(1Al) and T2m Q^4(2Al) sites decreases with disordering, causing a reduced spectral intensity in the −94 to −98 ppm range. The calculated second moments for both models are, however, significantly larger for the disordered samples than the observed values. These differences can be decreased either by choosing an ~3.5 ppm deshielding at ^{29}Si instead of 5 ppm for one Al for Si NNN substitution, or by the presence of additional short-range order beyond the avoidance of Al-O-Al linkages. For instance, a homogeneous dispersion of charge (Herrero *et al.*, 1989) would likely reduce the intensities of Q^4(0Al), Q^4(3Al) and Q^4(4Al) sites, thus decreasing the second moments.

Acknowledgements

This research was supported by NSF grant EAR90-04260. We thank Prof. E. Salje and Prof. G. Hovis for useful discussion of feldspar structures. Dr Randy Hughes and Dr Duane M. Moore provided help with the powder XRD refinement work. Dr Michael Carpenter and an anonymous reviewer provided helpful reviews.

Appendix

To calculate the relative intensities of the different possible Si Q^4(nAl) (n = 0,1,2,3,4) environments in alkali feldspars, we have used the following expressions. The equations assume that no Al-O-Al linkages are present (Loewenstein's Al-avoidance

Rule). In these equations, a, b, c and d are the Al contents of T1o, T1m, T2o and T2m, respectively.

T1o:

$$Q^4(4Al) = \frac{bcdd}{(1-a)^3}$$

$$Q^4(3Al) = \frac{2bcd(1-a-d) + ddc(1-a-b) + ddb(1-a-c)}{(1-a)^3}$$

$$Q^4(2Al) = [dd(1-a-b)(1-a-c) + bc(1-a-d)(1-a-d) + 2db(1-a-d)(1-a-c) + 2dc(1-a-d)(1-a-b)]/(1-a)^3$$

$$Q^4(1Al) = [2d(1-a-b)(1-a-c)(1-a-d) + b(1-a-c)(1-a-d)(1-a-d) + c(1-a-b)(1-a-d)(1-a-d)]/(1-a)^3$$

$$Q^4(0Al) = \frac{(1-a-d)(1-a-d)(1-a-c)(1-a-b)}{(1-a)^3}$$

T1m:

$$Q^4(4Al) = \frac{adcc}{(1-b)^3}$$

$$Q^4(3Al) = [2acd(1-b-c) + dcc(1-b-a) + acc(1-b-d)]/(1-b)^3$$

$$Q^4(2Al) = [ad(1-b-c)(1-b-c) + cc(1-b-a)(1-b-d) + 2ac(1-b-d)(1-b-c) + 2dc(1-b-a)(1-b-c)]/(1-b)^3$$

$$Q^4(1Al) = [2c(1-b-c)(1-b-a)(1-b-d) + a(1-b-d)(1-b-c)(1-b-c) + d(1-b-a)(1-b-c)(1-b-c)]/(1-b)^3$$

$$Q^4(0Al) = \frac{(1-b-a)(1-b-d)(1-b-c)(1-b-c)}{(1-b)^3}$$

T2o:

$$Q^4(4Al) = \frac{abdd}{(1-c)^3}$$

$$Q^4(3Al) = [2abd(1-c-d) + add(1-c-b) + bdd(1-c-a)]/(1-c)^3$$

$$Q^4(2Al) = [ab(1-c-d)(1-c-d) + 2ad(1-c-d)(1-c-b) + 2bd(1-c-a)(1-c-d) + dd(1-c-a)(1-c-b)]/(1-c^3$$

$$Q^4(1Al) = [a(1-c-b)(1-c-d)(1-c-d) + b(1-c-a)(1-c-d)(1-c-d) + 2d(1-c-d)(1-c-a)(1-c-b)]/(1-c)^3$$

$$Q^4(0Al) = \frac{(1-c-a)(1-c-b)(1-c-d)(1-c-d)}{(1-c)^3}$$

T2m:

$$Q^4(4Al) = \frac{aabc}{(1-d)^3}$$

$$Q^4(3Al) = \frac{2abc(1-d-a) + aab(1-d-c) + aac(1-d-b)}{(1-d)^3}$$

$$Q^4(2Al) = [aa(1-d-b)(1-d-c) + 2ab(1-d-a)(1-d-c) + 2ac(1-d-a)(1-d-b) + bc(1-d-a)(1-d-a)]/(1-d)^3$$

$$Q^4(1Al) = [2a(1-d-a)(1-d-b)(1-d-c) + b(1-d-a)(1-d-a)(1-d-c) + c(1-d-a)(1-d-a)(1-d-b)]/(1-d)^3$$

$$Q^4(0Al) = \frac{(1-d-a)(1-d-a)(1-d-b)(1-d-c)}{(1-d)^3}$$

References

Blasi, A., Brajkovic, A. and Blasi, C.D.P. (1984) Dry-heating conversion of low microcline to high sanidine via a one-step disordering process. *Bull. Mineral.*, **107**, 423–35.

Böhm, H. (1983) Modulated structures at phase transitions. *Amer. Mineral.*, **68**, 11–17.

Borg, I.Y. and Smith, D.K. (1969) *Calculated X-ray Powder Patterns for Silicate Minerals*. Geol. Soc. Amer., Mem. 122.

Burnham, C.W. (1962) LCLSQ-MARK VI, Least-squares refinement of crystallographic lattice parameters. *Carnegie Inst. Washington Yearb.*, **61**, 132–5.

Dal Negro, A., Pieri, R.D. and Quareni, S. (1978) The Crystal Structures of Nine K Feldspars from the Adamello Massif (Northern Italy). *Acta Crystallogr.*, **B34**, 2699–707.

Eggleton, R.A., and Buseck, P.R. (1980) The

Orthoclase-Microcline Inversion: A High-Resolution Transmission Electron Microscope Study and Strain Analysis. *Contrib. Mineral. Petrol.*, **74**, 123–33.

Engelhardt, G., Lippmaa, E. and Magi, M. (1981) Ordering of silicon and aluminum ions in the framework of NaX zeolites. A solid-state high-resolution Si NMR study. *J. Chem. Soc., Chem. Comm.*, 712–3.

Fyfe, C. A., Gobbi, G. C., Murphy, W. J., Ozubko, R. S. and Slack, D. A. (1984) Investigation of the contributions to the ^{29}Si MAS NMR line widths of zeolites and the detection of crystallographically inequivalent sites by the study of highly siliceous zeolites. *J. Amer. Chem. Soc.*, **106**, 4435–8.

Goldsmith, J.R. and Laves, F. (1954) The microcline-sanidine stability relations. *Geochim. Cosmochim. Acta*, **5**, 1–19.

Harris, M.J., Salje, K.H., Güttler B.K. and Carpenter, M.A. (1989) Structural States of Natural Potassium Feldspar: An Infrared Spectroscopic Study. *Phys. Chem. Minerals*, **16**, 649–58.

Hay, R.L., Lee, M., Kolata, D.R., Matthews, J.C. and Morton, J.P. (1988) Epidodic potassic diagenesis of Ordovician tuffs in the Mississippi Valley area. *Geology*, **16**, 743–7.

Herrero, C.P., Sanz, J. and Serratosa, J.M. (1989) Dispersion of Charge Deficits in the Tetrahedral Sheet of Phyllosilicates. Analysis from ^{29}Si NMR Spectra. *J. Phys. Chem.*, **93**, 4311–5.

Kim, Y.J. (1989) *Powder X-ray diffraction and transmission electron microscopic study of silicon-aluminum disordering in annealed Amelia albite and bancroft oligoclase*. Ms. thesis. Dept. of Geology, U. of Illinois.

Kirkpatrick, R.J. (1988) MAS NMR spectroscopy of minerals and glasses. In *Spectroscopic methods in mineralogy and geology*. (Hawthorne, F.C., ed.) *Reviews in Mineralogy*, **18**, 341–403.

Kirkpatrick, R.J., Kinsey, R.A., Smith, K.A., Henderson, D.M. and Oldfield, E. (1985) High resolution solid-state sodium-23, aluminum-27, and silicon-29 nuclear magnetic resonance spectroscopic reconnaissance of alkali and plagioclase feldspars. *Amer. Mineral.*, **70**, 106–23.

Kirkpatrick, R.J., Carpenter, M.A., Yang, W.-H. and Montez, B. (1987) ^{29}Si magic-angle NMR spectroscopy of low-temperature ordered plagioclase feldspars. *Nature*, **325**, 236–8.

Klinowski, J., Ramdas, S. Thomas, J.M., Fyfe, C.A. and Hartman, J.S. (1982) A re-examination of Si, Al ordering in zeolites NaX and NaY. *J. Chem. Soc., Faraday Trans.*, **2**. 78, 1025–50.

Kroll, H. (1971) Determination of Al, Si distribution in alkali feldspar from X-ray powder data. *Neues Jahrb. für Mineral., Mh.*, 91–4.

Kroll, H. (1973) Estimation of the Al, Si distribution of feldspars from the lattice translations Tr[110] and Tr[1$\bar{1}$0]. I. Alkali feldspars. *Contrib. Mineral. Petrol.*, **39**, 141–56.

Kroll, H. and Knitter, R. (1991) Al, Si exchange kinetics in sanidine and anorthoclase and modeling of rock cooling paths. *Amer. Mineral.*, **76**, 928–41.

Kroll, H. and Ribbe, P.H. (1983) Lattice parameters, composition and Al,Si order in alkali feldspars. In *Feldspar Mineralogy*. (P.H. Ribbe, ed.) *Review in Mineralogy*, 2, 2nd edition, MSA, 57–99.

Lippmaa, E., Magi, M. Samoson, A. Engelhardt, G. and Grimmer, A.-R. (1980) Structural studies of silicates by solid-state high-resolution Si NMR. *J. Amer. Chem. Soc.*, **102**, 4889–93.

Loewenstein, W. (1954) The distribution of aluminum in the tetrahedra of silicates and aluminates. *Amer. Mineral.*, **39**, 92–6.

Phillips, B.L., Allen, F.M. and Kirkpatrick, R.J. (1987) High-resolution solid-state ^{27}Al NMR spectroscopy of Mg-rich vesuvianite. *Amer. Mineral.*, **72**, 1190–4.

Phillips, B.L., Kirkpatrick, R.J. and Hovis, G.L. (1988) ^{27}Al, ^{29}Si and ^{23}Na MAS NMR Study of an Al, Si Ordered Alkali Feldspar Solid Solution Series. *Phys. Chem. Minerals*, **16**, 262–72.

Putnis, A. and Angel, R.J. (1985) Al, Si Ordering in Cordierite Using 'Magic Angle Spinning' NMR. II. Models of Al, Si Order from NMR Data. *Phys. Chem. Minerals*, **12**, 217–22.

Putnis, A. and Bish, D.L. (1983) The mechanism and kinetics of Al, Si ordering in Mg-cordierite. *Amer. Mineral.*, **68**, 60–5.

Putnis, A., Salje., E., Redfern, S.A.T., Fyfe, C.A. and Strobl, H. (1987) Structural States of Mg-Cordierite I: Order Parameters from Synchrotron X-Ray and NMR Data. *Phys. Chem. Minerals*, **14**, 446–54.

Ramdas, S. and Klinowski, J. (1984) A simple correlation between isotropic ^{29}Si-NMR chemical shifts and T-O-T angles in zeolite frameworks. *Nature*, **308**, 521–3.

Ribbe, P.H. (1983) Aluminum-silicon order in feldspars: domain textures and diffraction patterns. In *Feldspar Mineralogy*. (Ribbe P.H. ed.) *Reviews in Mineralogy*, 2, 2nd edition, MSA, 21–55.

Salje, E. (1987) Structural States of Mg-Cordierite II: Landau Theory. *Phys. Chem. Minerals.*, **14**, 455–60.

Samoson, A. (1985) Satellite Transition High-Resolution NMR of Quadrupolar Nuclei in Powders. *Chem. Phys. Letts.*, **119**, 29–32.

Sherriff, B.L. and Hartman J.S. (1985) Solid-state high-resolution ^{29}Si NMR of feldspars: Al-Si disorder and the effects of paramagnetic centers. *Canad. Mineral.*, **23**, 205–12.

Sipling, P.J. and Yund, R.A. (1974) Kinetics of Al/Si disordering in alkali feldspars. In *Geochemical transport and kinetics*. (A.W. Hofmann *et al.* eds.) Carnegie Institute of Washington Publication 634, 185–93.

Slichter, C.P. (1990) *Principles of Magnetic Resonance.*

3rd ed. Springer-Verlag.

Smith, J.V. (1974) *Feldspar Minerals*, Vol. 1 and Vol. 2, Springer-Verlag, New York Heidelberg Berlin.

Smith, J.V., Blackwell, C.S. and Hovis, G.L. (1984) NMR of albite-microcline series. *Nature*, **309**, 140–2.

Smith, K.A., Kirkpatrick, R.J., Oldfield, E. and Henderson, D.M. (1983) High-resolution silicon-29 nuclear magnetic resonance spectroscopic study of rock-formation silicates. *Amer. Mineral.*, **68**, 1206–15.

Stewart, D.B. and Ribbe, P.H. (1969) Structural explanation for variations in cell parameters of alkali feldspar with Al/Si ordering. *Amer. J. Sci.*, **267-A**, 444–62.

Wright, T.L. and Stewart, D.B. (1968) X-ray and optical study of alkali feldspar I. Determination of composition and structural state from refined unit-cell parameters and 2V. *Amer. Mineral.*, **53**, 38–87.

Xu, H., Luo, G., Hu, M. and Chen, J. (1989) HRTEM Study of The Superlattice Orthoclase. *Acta Physica Sinica*, **38**, 1527–9.

Yang, W., Kirkpatrick, R.J. and Henderson, D.M. (1986) High-resolution ^{29}Si, ^{27}Al and ^{23}Na NMR spectroscopic study of Al-Si disordering in annealed albite and oligoclase. *Amer. Mineral.*, **71**, 712–26.

[*Revised manuscript received 20 September 1993: revised 12 February 1994*]